

# On the Crushing Mechanics of Thin-Walled Structures

**T. Wierzbicki**

Professor of Mechanics,  
Department of Ocean Engineering,  
Massachusetts Institute of Technology,  
Cambridge, Mass. 02139

**W. Abramowicz**

Assistant Professor,  
Institute of Fundamental  
Technological Research,  
Swietokrzyska 21,  
00-049 Warsaw, Poland

*A self-consistent theory is presented which describes the crushing behavior of a class of thin-walled structures. Assuming a rigid-plastic material and using the condition of kinematic continuity on the boundaries between rigid and deformable zones, a basic folding mechanism is constructed. This mechanism closely reproduces all the main features of folds and wrinkles actually observed on typical crumpled sheet metal structures. Calculations based on the energy balance postulate show that two-thirds of the plastic energy is always dissipated through inextensional deformations at stationary and moving plastic hinge lines. The extensional deformations are confined to relatively small sections of the shell surface but they account for the remaining one-third of the dissipated energy. The theory is illustrated by application to the problem of progressive folding of thin-walled rectangular columns. A good correlation is obtained with existing experimental data as far as the mean crushing force and the geometry of the local collapse mode is concerned.*

## 1 Introduction

Thin-walled structures are capable of carrying substantial loads for deflections far beyond those corresponding to ultimate or buckling loads. From the point of view of energy absorption characteristics of compressed members, one is mainly interested in deflections that exceed by two orders of magnitude the shell thickness and become comparable to the linear dimension of the structure. At the same time consideration of initial peak load is important only to the extent that the process of reaching this load may impose a certain mode of collapse.

Very large deflections can be accommodated by sheet metal structures through the formation of a complicated pattern of folds and wrinkles. A distinctive feature of such a deformation mechanism is that the strain energy (in the case of elastic shells) or the rate of energy dissipation (in the case of plastic shells) is concentrated over relatively narrow zones, while the remainder of the structure undergoes a rigid body motion. This is in sharp contrast with buckling or post-buckling behavior of plates or shells where small perturbations around a predominantly compressive state lead to a more or less uniform strain distribution.

Some further interesting observations can be made about the crumpling process. The fold lines, which actually form a double curvature surface, always lie in a certain plane. One radius of curvature of the "fold line" is small and comparable to the gauge thickness while the other is much larger. Once the

local buckling wave is formed in the shell, its length stays essentially unchanged while the amplitude grows as the deformation progresses.

All these features of the structural response are local and thus, to a certain degree, are independent of the scale or type of the problem. This means that one should be able to describe the mechanics of the crushing process at this local level. Calculations of the crushing resistance of typical components of automobile, aircraft, or ship structures will then follow.

The progressive folding of box columns was studied among others by Johnson et al. [1], Ohokubo et al. [2], and one of the present author [3], under the assumption of purely inextensional deformation modes with stationary or moving hinge lines. On the other hand, for axially symmetric problems such as tube inversion [4], crumpling of cylindrical shells in the so-called crinkling deformation mode [5], and crushing of rotationally symmetric shells [6,7], a predominantly extensional type of deformation was assumed. In the present paper these two approaches are combined to develop a theory of the crushing behavior of a certain class of shells.

A kinematic method of plasticity will be used, suitably generalized to large deformation problems. The method consists of constructing a kinematically admissible solution, with at least three degrees of freedom (three free parameters) around a simple one-degree-of-freedom folding mechanism.

## 2 Assumptions

The shape of the plastic collapse mode with large local strains and curvatures can be assumed a priori on the basis of experimental observations. Alternatively, the folding mechanisms can be systematically developed from a set of basic assumptions in conjunction with the continuity conditions at the propagating hinge lines. Here, the latter ap-

Contributed by the Applied Mechanics Division and presented at the Winter Annual Meeting, Boston, Mass., November 13-18, 1983 of THE AMERICAN SOCIETY OF MECHANICAL ENGINEERS.

Discussion on this paper should be addressed to the Editorial Department, ASME, United Engineering Center, 345 East 47th Street, New York, N.Y. 10017, and will be accepted until two months after final publication of the paper itself in the JOURNAL OF APPLIED MECHANICS. Manuscript received by ASME Applied Mechanics Division, April, 1982; final revision, April, 1983. Paper No. 83-WA/APM-12.

Copies will be available until July, 1984.

proach is used since it will shed more light on the crushing process of thin-walled structures. The following assumptions are made:

(1) The structure consists initially of planar surface elements. This assumption restricts the class of the considered problem. For example, box beams and columns, plate intersections, cellular structures, stiffened panels etc., all fall within the considered class. The method may also be applied to curved shells that are approximated by a system of flat plates.

(2) The material is regarded as rigid-perfectly plastic with a constant value of the flow stress  $\sigma_0$ . Since large plastic strains are present in areas of high curvature, elastic effects can be neglected and  $\sigma_0$  can be thought of as an average flow stress. Strain hardening and strain rate sensitivity can be accounted for in the present formalism at the expense of considerably more complicated calculations.

(3) The length of the local buckling wave  $2H$  remains constant during the formation of each buckle or fold. This is true in many practical problems. Usually, the mode of collapse of a thin-walled structure is either imposed by initial imperfections or is dictated by initial elastic or plastic buckling modes. The fact that this wavelength is not subjected to any major changes later in the post-buckling process means that there must be a way of determining  $H$  from the energy consideration in the plastic range. We will explore this possibility further in the paper.

(4) The constraints imposed on the crushing process by the boundary and symmetry conditions are forcing the fold lines to move through the material. The consideration of folding about stationary (straight or curved) hinge lines is in general much easier. Such collapse mechanisms are possible to develop only if sufficient freedom is left for the boundaries to deform. This problem has been analyzed in the literature, cf. [1] and thus will not be considered here.

### 3 Analysis of Discontinuities

The conditions on the boundaries between rigid and deforming zones will now be examined. Consider a curved discontinuity line  $\Gamma$  moving down the middle surface of the shell  $\chi$  with the velocity  $V_n$ . The hinge line is defined by the surface vector  $\mathbf{n}$  normal to  $\Gamma$ . The line  $\Gamma$  is dividing the surface  $\chi$  into two separable parts, the deformed part  $(+)_\chi$  behind  $\Gamma$ , which is subjected to plastic deformations and the undeformed part  $(-)_\chi$  in front of  $\Gamma$ . Denote by  $f$  any vector field defined over the surface  $\chi$ . In particular  $\mathbf{f}$  can be regarded as a displacement vector  $\mathbf{f} = \{u^\alpha, u^3\}$ , in the local coordinate system  $(x^\alpha, x^3)$ .

The conditions of kinematic continuity of  $f$  across  $\Gamma$  take the form

$$[\dot{f}^i] + V_n [f^i |_\alpha] n^\alpha = 0 \quad i = \{1, 2, 3\} \quad (3.1)$$

$$[f^i |_\alpha] + V_n \{ [f^i |_{\beta\gamma}] n^\beta n^\gamma \} n_\alpha = 0 \quad \alpha, \beta, \gamma = \{1, 2\} \quad (3.2)$$

where the brackets denote discontinuities, if any of the enclosed quantities across  $\Gamma$ , i.e.,  $[\eta] = +\eta - -\eta$ , and  $V_n$  is the velocity of the hinge line in  $\mathbf{n}$  direction. These equations can be obtained from general continuity conditions for a three-dimensional continuum formulated, for example, in [8] if the first and second gradient of the function  $f$  is replaced by the corresponding covariant differentiation.

In the case of rotationally symmetric shells the hinge line becomes a circle and each of the continuity conditions (3.1) and (3.2) yields only one scalar equation in the meridional plane

$$[\dot{f}] + V_n [f_{,\alpha}] = 0 \quad (3.3)$$

$$[\dot{f}_{,\alpha}] + V_n [f_{,\alpha\alpha}] = 0 \quad (3.4)$$

where  $[\dot{f}_{,\alpha}]$  is a jump of the rate of rotation and  $[f_{,\alpha\alpha}]$  is the corresponding jump in the principle (meridional curvature).

Assuming that  $f$  and  $\dot{f}$  are continuous across  $\Gamma$ , equation (3.3) shows that the slope  $f_{,\alpha}$  can be discontinuous only across stationary hinge lines, for which  $V_n = 0$ . Similar results valid for beams and flat circular plates were obtained earlier by Hopkins [9] and Prager [10].

Two special cases of the general equations are of interest to us. Let a circular hinge  $\Gamma$  move down a cylindrical surface of the radius  $R$ . The curvature and rate of rotation vanish in front of  $\Gamma$  and behind  $\Gamma$  are denoted, respectively, by  $f_{,\alpha\alpha} = \kappa = 1/b$ ,  $\dot{f}_{,\alpha} = \dot{\theta}$ . Equation (3.4) says that such a line of discontinuity is leaving behind a curved surface, defined by

$$\dot{\theta} + V/b = 0 \quad (3.5)$$

In a small neighborhood of  $\Gamma$  this is the equation of a toroidal surface with the small radius  $b$  and large radius  $a = R + b$ , Fig. 1(a).

Consider now a straight hinge line moving down a plane surface. Equation (3.2) yields a condition analogous to (3.5) but its interpretation is different. A translating or rotating hinge lines is sweeping, respectively, a cylindrical or conical surface of the radius  $b$ , Fig. 1(b,c). Reversing the directions of motion, a converse statement is true. A toroidal surface is transformed into a cylinder while a cylindrical or conical surface becomes a plane.

### 4 Basic Folding Mechanism

Following assumption 1, consider a typical hinge line formed by an intersection of two plane surface elements which initially were of the height  $H$ . Referring to Fig. 2 we see that upon compression, the hinge line, originally positioned at

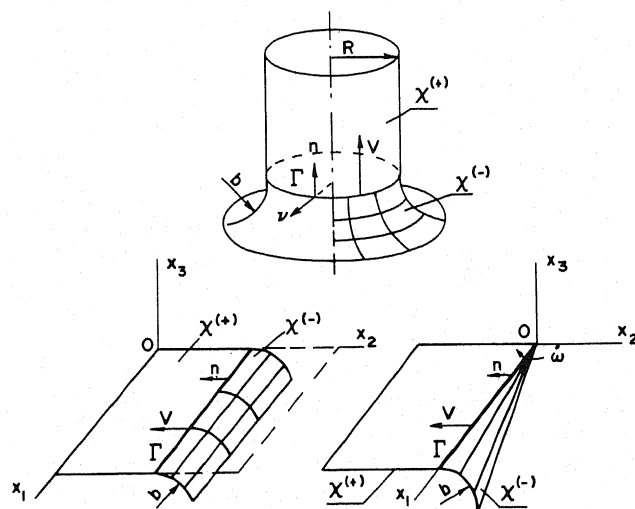


Fig. 1 Kinematic continuity at straight and curved propagating hinge lines

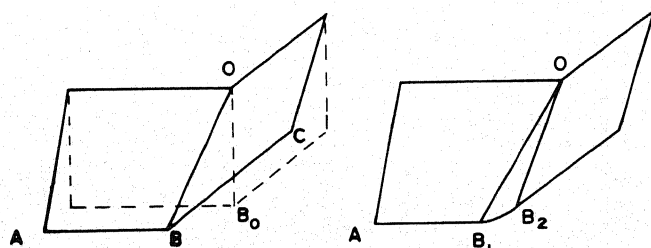


Fig. 2 Kinematically inadmissible and admissible folding mechanisms

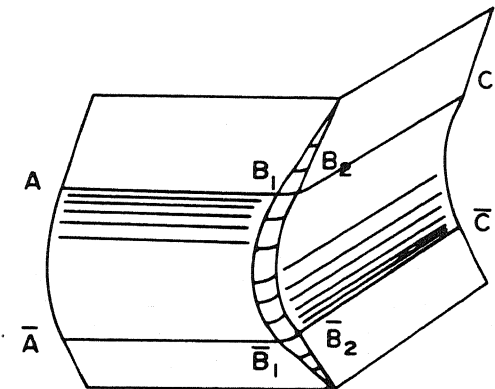
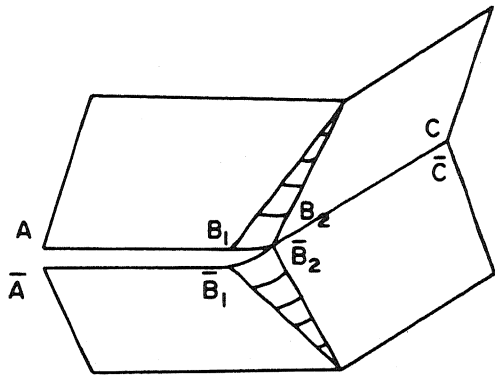


Fig. 3 (a) Assembling two asymmetric modes with material discontinuity; and (b) a fully consistent collapse mechanism

$OB_0$ , has moved to a new position  $OB$ . Such a mode of deformation is kinematically inadmissible since it incorporates a discontinuity in the slope across the moving hinge line. A consistent collapse mechanism is obtained by introducing two rotating hinge lines. The first line is imposing a curvature and this line is followed by another one that is removing the curvature back to zero. The resulting mode thus consists of two flat trapezoidal elements continuously joined by a section of a conical surface, Fig. 3. When two identical modes described in the foregoing are assembled, a stationary hingeline  $BC$  is formed across which the slope discontinuity is admissible. This however results in a material discontinuity over the remaining part of the joint line. The opening increases from  $B_2$  to  $B_1$  and then is held constant along  $BA$ , Fig. 3. The width of the gap indicates how much extension or compression would be required to ensure full geometric compatibility. This difficulty could be overcome by inserting a section of a cylindrical surface between the two deforming elements along the horizontal edge  $CAB$ , Fig. 3. As the deformation progresses, each of the horizontal lines split now into two hinges moving in opposite directions. According to the continuity condition (3.5) the central region bounded by four moving circular arcs must form a section of a toroidal surface. The deformation mode consisting of four trapezoidal elements, a section of two horizontal cylindrical surfaces, two inclined conical surfaces, and a section of a toroidal surface will be called a *basic folding mechanism*.

**Velocity and Strain Rate Fields.** The global geometry of four intersecting fold lines is shown in Fig. 4. The initial geometry of the compressed element is defined by the height  $2H$ , total width  $C$ , which is the length of the segments  $AB$  and  $BC$ , and the angle  $2\psi_0$  between two adjacent plates. The current geometry is described either by the crushing distance  $\delta$  or the angle of rotation of the side panels  $\alpha$  or the horizontal

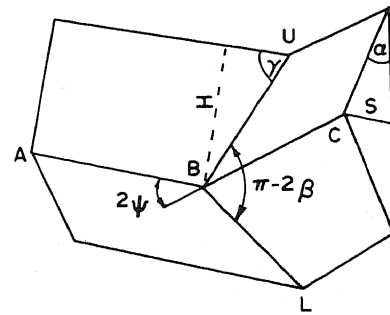


Fig. 4 Global geometry of the basic folding mechanism

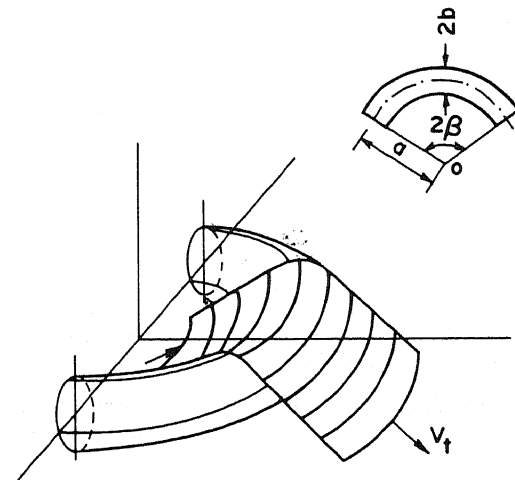


Fig. 5 Plastic flow of a metal sheet through a toroidal surface

displacements of the point  $B$ . These quantities are mutually related by

$$\delta = 2H(1 - \cos \alpha) \quad (4.1)$$

$$S = H \sin \alpha \quad (4.2)$$

The other two angles  $\gamma$  (in the plane  $ABU$ ) and  $2\beta$  (in the plane  $UBL$ ) are related to  $\psi_0$  and  $\alpha$  through

$$\tan \gamma = \frac{\tan \psi_0}{\sin \alpha}, \quad \tan \beta = \frac{\tan \gamma}{\sin \psi_0} \quad (4.3)$$

The motion of the element is described by the relative velocity of the upper and lower edges (Points  $U$  and  $L$ )

$$\dot{\delta} = 2H(\sin \alpha) \dot{\alpha} \quad (4.4)$$

and the horizontal velocity of the point  $C$

$$V = \dot{S} = H(\cos \alpha) \dot{\alpha} \quad (4.5)$$

A central point in the present paper is the analysis of a continuous deformation field leading to extensional deformations in the localized zones. The velocity field in the section of a toroidal shell can be determined in the fixed coordinate system or more conveniently in the moving coordinate system referred to the global collapse mode.

On subtracting the convective part of the velocity field it can be easily shown (cf. for example [19]), that the local motion of the shell middle-surface in the considered zone is nothing else but a radial flow of the material points over the toroidal surface with the tangential velocity  $V_t$ . This velocity is related to the horizontal velocity  $V$  by Fig. 5.

$$V_t = \dot{\omega}b = V/\tan \psi_0 \quad (4.6)$$

Let us introduce a local coordinate system  $\{\theta, \phi, x^3\}$  where  $\theta$  and  $\phi$  denote, respectively, meridional and circumferential coordinates of the toroidal surface. Assuming inextensibility of the shell in the meridional direction ( $\lambda_\theta = 1$ ), the velocity

vector in this system of coordinates has the following components

$$\mathbf{v} = \{\dot{\omega}b, 0, 0\} \quad (4.7)$$

where  $\dot{\omega}$  denotes the angular velocity of the flow.

It is natural to introduce a consistent Eulerian description of the plastic flow. The formulated problem is geometrically nonlinear in strains and displacements. However, the formula for the velocity strain is linear. The velocity field (4.7) gives rise to the following components of the rate of extension  $\dot{\lambda}_{\alpha\beta}$  and rate of curvature  $\dot{\kappa}_{\alpha\beta}$ , in the continuous deformation field where  $\alpha, \beta = \theta, \phi$  (for details of derivation see, for example, reference [12])

$$\dot{\lambda}_{\alpha\beta} = \begin{bmatrix} 0 & 0 \\ 0 & \dot{\lambda}_{\phi\phi} \end{bmatrix}, \quad \dot{\kappa}_{\alpha\beta} = \begin{bmatrix} 0 & 0 \\ 0 & \dot{\kappa}_{\phi\phi} \end{bmatrix} \quad (4.8)$$

where

$$\dot{\lambda}_{\phi\phi} = -\frac{\dot{\omega}b \sin \theta}{r}, \quad \dot{\kappa}_{\phi\phi} = -\frac{\dot{\omega}a \sin \theta}{r^2} \quad (4.9)$$

There is also a jump in the curvature rate across the two circular hinge lines

$$[\dot{\kappa}_{\theta\theta}] = \dot{\theta} = V_t/b \quad (4.9a)$$

In the preceding formulas  $a$  and  $b$  denote, respectively, larger and smaller radius of the toroidal surface and  $r$  is a current position of the point with  $\theta$  coordinate with respect to the axis of symmetry  $r = b \cos \theta + a$ .

**Incompressibility Condition.** The general theory, on which the derivation of equations (4.8) and (4.9) was based, does not pose any restrictions as to the change of the shell thickness during the deformation process. Since the material is rigid-plastic, we can calculate the change of thickness from the incompressibility condition. In view of the property  $\lambda_\theta = 1$ , this conditions reads

$$\lambda_\phi \lambda_x = 1 \quad (4.10)$$

This condition can be written in an integral form which related local wall thickness to the current radius of the toroidal surface,  $h_0 r_0 = hr$  where  $h_0$  is the initial thickness of the shell and  $r_0 = a + b \sin \psi$ .

## 5 Energy Dissipation

The rate of energy dissipated in the crushing process results from the continuous and discontinuous velocity fields

$$\dot{E}_{int} = \int_S (M^{\alpha\beta} \dot{\kappa}_{\alpha\beta} + N^{\alpha\beta} \dot{\lambda}_{\alpha\beta}) dS + \int_L M_0 \dot{\theta} d\ell \quad (5.1)$$

where  $\dot{\alpha}_{\alpha\beta}$  and  $\dot{\lambda}_{\alpha\beta}$  are given by (4.8) and (4.9) and the Cauchy stress tensor is used in the definition of stress resultants  $N^{\alpha\beta}$  and stress couples  $M^{\alpha\beta}$ . Note that both the extent of continuous plastic deformations  $S$  and the length of hinge lines  $L$  increase as the deformation progresses. Consider now the first integral in (5.1).

Each element of the shell subjected to plastic flow undergoes a finite rotation from  $\theta_1 = \pi/2 + \psi$  to  $\theta_2 = \pi/2 - \psi$ . It seems appropriate here to introduce the corotational definition of the yield condition discussed, for example, in [12]. The yield condition is described by the same function of the components of generalized stresses  $F(M^{\alpha\beta} N^{\alpha\beta}) = 0$ , independent of the actual configuration, i.e., the coordinates  $\{\theta, \phi\}$ . The form of the function  $F$  would then be formally analogous to that describing a similar problem with infinitesimal deformations. In the case of rotationally symmetric shells with only two nonvanishing components of the generalized strain rate tensor, the yield condition has the form

$$\left| \frac{M_{\phi\phi}}{M_0} \right| + \left( \frac{N_{\phi\phi}}{N_0} \right)^2 = 1 \quad (5.2)$$

where  $M_0 = 1/4 \sigma_0 h^2$ ,  $N_0 = \sigma_0 h$  and  $h$  represents the current, variable shell thickness. The preceding equation in conjunction with the associated flow rule suffices to determine uniquely the continuous rate of energy dissipation.

The surface element in (5.1) is expressed as

$$dS = r d\phi b d\theta \quad (5.3)$$

and the limits of integration are

$$\frac{\pi}{2} - \psi \leq \theta \leq \frac{\pi}{2} + \psi \quad (5.4)$$

$$-\beta < \phi < \beta$$

where  $2\beta$  is a central angle of toroidal section, variable with the process, see Fig. 5, and the angle  $\psi$  is linearly increasing with  $\phi$  from  $\psi_0$  to  $\pi/2$  according to

$$\psi = \psi_0 + \frac{\pi - 2\psi_0}{\pi} \phi \quad (5.4a)$$

In the most general case of variable thickness and nonlinear yield condition, the surface integral in (5.1) can be evaluated and expressed in terms of elementary functions as shown in [13]. However, the resulting expression is too complicated for our purposes.

The effect of variable thickness is small except for problems in which the ratio  $\eta = b/a$  is relatively large, for example an outside-in tube inversion. We will restrict our analysis to small  $\eta$  and treat  $h$  as constant. We will also approximate (5.2) by a square yield locus, circumscribed on the parabola. The first integral in (5.1) is then reduced to

$$\dot{E}_1 = \int_{-\beta}^{\beta} b \left\{ \int_{\pi/2-\psi}^{\pi/2+\psi} \left[ M_0 \frac{\dot{\omega} a \sin \theta}{r^2} + N_0 \frac{\dot{\omega} b \sin \theta}{r} \right] r d\theta \right\} d\phi$$

The first integration can be easily performed to give

$$\dot{E}_1 = \int_{-\beta}^{\beta} \left\{ 2\dot{\omega} b^2 N_0 \sin \psi + \dot{\omega} b M_0 \frac{1}{\eta} \ln \left( \frac{1 + \eta \sin \psi}{1 - \eta \sin \psi} \right) \right\} d\phi \quad (5.5)$$

For small  $\eta$  the second term in the integrand of (5.5) can be expanded in power series. Retaining only the linear term, this formula reduces to

$$\dot{E}_1 = \int_{-\beta}^{\beta} \{ 2\dot{\omega} b \sin \psi [N_0 b + M_0] \} d\phi \quad (5.6)$$

Note that the dependence of the solution on the larger radius  $a$  is weak and disappears altogether for small  $\eta$ . The first term in the integrand of (5.6) represents the contribution of circumferential extension while the second term the contribution of continuous bending (change of circumferential curvature). Since  $b$  is always greater than the thickness of the shells and in most cases is of the order of  $b = 4h$ , the continuous bending does not contribute much to the rate of energy dissipation in regions of continuous deformation and thus can be neglected in simplified calculations. Sawczuk and one of the present authors [13] studied the ratio  $\kappa\phi\phi/\dot{\lambda}_{\phi\phi}$  and found that for small  $\eta$  the stress profile is reduced to a single point on the yield condition  $M = 0$ ,  $N = N_0$ . The second integration can be performed with the help of (4.5), (4.6), and (5.4a) and the result is

$$\dot{E}_1 = \frac{4N_0 b H \pi}{(\pi - 2\psi_0) \tan \psi_0} \cos \alpha \left\{ \sin \psi_0 \sin \left( \frac{\pi - 2\psi_0}{\pi} \right) \beta + \cos \psi_0 \left[ 1 - \cos \left( \frac{\pi - 2\psi_0}{\pi} \right) \right] \beta \right\} \alpha \quad (5.6a)$$

Integrating now (5.6a) over the whole deformation process, the work done on a complete folding of the element through the angle  $\pi/2$  is

$$E_1 = 4Hb N_0 I_1(\psi_0) = 16 M_0 Hb/h I_1(\psi_0) \quad (5.7)$$

where  $I_1$  is defined by

$$I_1(\psi_0) = \frac{\pi}{(\pi - 2\psi_0)tg\psi_0} \int_0^{\pi/2} \cos \alpha \left\{ \sin \psi_0 \sin \left( \frac{\pi - 2\psi_0}{\pi} \right) \beta + \cos \psi_0 \left[ 1 - \cos \left( \frac{\pi - 2\psi_0}{\pi} \right) \beta \right] \right\} d\alpha \quad (5.7a)$$

Since, according to (4.3), the angle  $\beta$  is a function of  $\alpha$ , the preceding integral is a known function of the angle  $\psi_0$ .

The second integral in the expression (5.1) represents the internal energy dissipation by the discontinuous velocity field on the horizontal and inclined hinge lines. Consider first the horizontal hinges. The length of each horizontal hinge line is constant and equal to  $C$ . Because the hinge line is split, there will be two such hinge lines in the basic folding mechanism. The contribution of this mechanism is

$$\dot{E}_2 = 2M_0 C \dot{\theta} = 2M_0 C \dot{\alpha}, \quad (5.8)$$

or after integration over the whole process

$$E_2 = 2 \int_0^{\pi/2} M_0 C d\alpha = \pi M_0 C \quad (5.9)$$

Additional energy will be dissipated if the horizontal boundary condition of the basic folding mechanisms were of the clamped rather than simply supported type.

The length of the inclined hinge lines changes in the process and is equal approximately to

$$L = 2H / \sin \gamma \quad (5.10)$$

In more exact calculations, the large radius of the toroidal surface would enter the expression for  $L$ . The inclined hinge lines consist of two segments of straight lines and an arc of the circle defined by the radius  $r_0$  and central angle  $2\beta$ .

The discontinuity in the rate of rotation in the meridional direction is constant along  $L$  and equal to

$$\dot{\theta} = V_1 / b \quad (5.11)$$

Since there are two inclined hinge lines (one imposing and one removing the curvature), the energy dissipation in this deformation mechanism becomes

$$\dot{E}_3 = 2M_0 L \dot{\theta} = 4M_0 \frac{H^2}{b} \frac{1}{tg\psi_0} \frac{\cos \alpha}{\sin \gamma} \quad (5.12)$$

where the angle  $\gamma$  is related to  $\alpha$  by means of (4.3). The corresponding work done upon complete folding, obtained from (5.12) is

$$E_3 = 4M_0 I_3(\psi_0) H^2 / b \quad (5.13)$$

where  $I_3$  is defined by

$$I_3(\psi_0) = \frac{1}{tg\psi_0} \int_0^{\pi/2} \frac{\cos \alpha}{\sin \gamma} d\alpha$$

The rate of external work done on compressing the basic folding mechanisms is

$$\dot{E}_{\text{ext}} = P \dot{\delta} = P \cdot 2H(\sin \alpha) \dot{\alpha} \quad (5.14)$$

while the total plastic work required to crush the element through the distance  $2H$  equals

$$E_{\text{ext}} = 2PH \quad (5.15)$$

## 6 Properties of the Solution

Having identified the basic mechanisms of plastic dissipation one can proceed now to the calculation of the crushing resistance of thin-walled structural members that can be assembled from the basic folding mechanism. Some interesting observations can be made at the general level without specifying any particular type of a structure.

The instantaneous crushing force  $P$  is defined by the requirement that the rate of internal and external energy dissipation be equal,  $\dot{E}_{\text{ext}} = \dot{E}_1 + \dot{E}_2 + \dot{E}_3$ . This is equivalent to assuming a global equilibrium in the shell. However, locally the equilibrium may be violated. The terms  $\alpha$  drops out from both sides of the equation and an expression is obtained for the force-shortening characteristics of the compressed member. This expression involves two unknown geometrical parameters  $H$  and  $b$  (the third parameter  $a$  disappeared in simplified calculations). To determine these parameters, consider the mean crushing force  $P_m$ , defined by the balance of total energies  $E_{\text{ext}} = E_1 + E_2 + E_3$ . It is easy to see from (5.7), (5.9), and (5.13) that the general form of the formula for  $P_m$  is

$$\frac{P_m}{M_0} = A_1 \frac{b}{h} + A_2 \frac{C}{H} + A_3 \frac{H}{b} \quad (6.1)$$

where numerical values of the parameters  $A_1$ ,  $A_2$ , and  $A_3$  are known and depend on the type of problem.

It seems reasonable to postulate that the collapse mechanism, which activates and persists in the course of the crushing process leads to the least possible amount of the mean crushing force. Indeed, the minimum of (6.1) does exist with respect to both  $H$  and  $b$ . The unknown parameters can thus be determined from the set of equations

$$\frac{\partial P_m}{\partial H} = 0, \quad \frac{\partial P_m}{\partial b} = 0 \quad (6.2)$$

Postulating a similar condition for the instantaneous rather than mean crushing force would be appropriate only if an additional dissipation mechanism, responsible for the change in the wavelength  $H$  was considered and if random or buckling-induced imperfections were accounted for. Without these measures, the optimality condition for the rate of energy dissipation would lead to the variable wavelength, which contradicts the assumption 3. This interesting problem is discussed at length in [14].

The solution to equation (6.2) is

$$b = \sqrt[3]{A_2 A_3 / A_1^2} \sqrt[3]{C h^2}, \quad H = \sqrt[3]{A_2^2 / A_1 A_3} \sqrt[3]{C^2 h}, \quad (6.3)$$

Substituting (6.3) back into (6.1) we obtain

$$\frac{P_m}{M_0} = 3 \sqrt[3]{A_1 A_2 A_3} \sqrt[3]{C / h} \quad (6.4)$$

This is an extremely interesting and important result. It shows that all three major mechanisms of energy dissipation discussed in the paper, contribute equally to the total energy dissipation, irrespective of the actual numerical values of the coefficient  $A_1$ ,  $A_2$ , and  $A_3$ . This property follows directly from the coupling effect of the continuous deformations in the toroidal surface. In particular, we can see that two-thirds of the plastic energy is always dissipated through inextensional deformations at stationary and moving plastic hinge lines. The extensional deformations, confined to the small fraction of the total area of the shell, are responsible for the remaining one-third of the dissipated energy.

The expression (6.3) can be used in conjunction with the rate of energy balance equation to derive the load-deflection characteristics of the member. Its general form is

$$P(\delta) = P_m f(\delta) \quad (6.5)$$

and a detailed discussion of its validity is presented in [14].

## 7 Applications, Crushing of a Box Column

This problem received a great deal of attention in the literature in view of its obvious application in controlling the process of energy absorption by automobile bodies during a front or rear-end collision.

The experimentally observed collapse mechanism of a rectangular column can be modeled with a good accuracy by an assembly of four basic folding mechanisms, each of the length  $C$ . The crumpling process of a rectangular tube is progressive, each new fold is being formed after the previous one is completed, Fig. 6. The corresponding force-shortening characteristics exhibits fluctuations around a mean value with peaks and valleys positioned at regular intervals  $2H$ , Fig. 7. The energy absorption of the member is thus well characterized by the mean crushing for  $P_m$ . The dimensions of the rectangular cross section  $c \times d$ , the wall thickness  $h$ , the angle  $2\psi_0 = 90$  deg between plates, and the flow stress  $\sigma_0$  are all considered as known. The sought-off quantities are the mean crushing force  $P_m$ , the wavelength  $H$ , and the rolling radius  $b$ . The values of the integrals, corresponding to  $\psi_0 = \pi/4$  are  $I_1 = 0.58$ ,  $I_3 = 1.11$ .

Since a section of the rectangular tube is composed of four basic folding elements, all energies, calculated in Section 5 should be multiplied by four. Moreover, because of clamped boundary conditions at horizontal edges, the energy  $E_2$  should be doubled. The energy balance equation yields

$$2H P_m = M_0 \left\{ 64 I_1 \frac{bH}{h} + 8\pi C + 16 I_3 \frac{H^2}{b} \right\} \quad (7.1)$$

where  $C = 1/2 (c+d)$ . By comparing (7.1) with (6.1), the

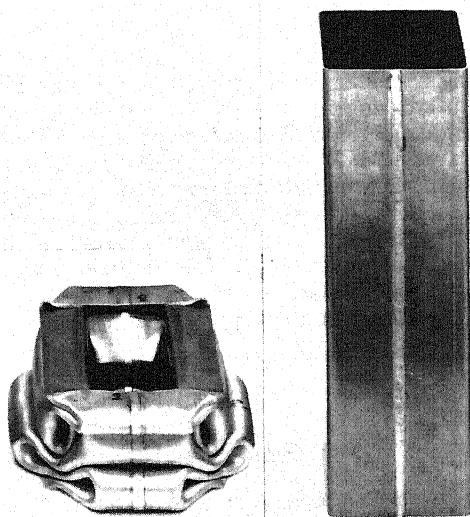


Fig. 6 Typical view of the fully crushed rectangular box column

values of the coefficients are found to be  $A_1 = 32I_1 = 18.56$ ,  $A_2 = 4\pi$ ,  $A_3 = 8I_3 = 8.91$ . The solution for  $H$  and  $b$  calculated from (6.3) is

$$H = 0.983 \sqrt[3]{hC^2}, \quad b = 0.687 \sqrt[3]{h^2 C} \quad (7.2)$$

while the expression (6.4) for the mean crushing force becomes

$$\frac{P_m}{M_0} = 38.27 \sqrt[3]{\frac{C}{h}} \quad (7.3)$$

In particular, for a square tube, for which  $c=d=C$ , a simple and practical formula is obtained

$$P_m = 9.56 \sigma_0 h^{5/3} C^{1/3} \quad (7.4)$$

where in transforming of (7.3) into (7.4) a definition of the fully plastic moment was used.

Attention is drawn here to the term  $h^{5/3}$ . In all known solutions to this problem, based on inextensional collapse modes, the crushing force was proportional to  $h^2$ , [2, 3]. If pure extensions were present in sheet metal structures, the crushing force would be proportional to  $N_0 = \sigma_0 h$ . In the present analysis the ratio of bending and extension is 2:1 and this property is also reflected in the value of the exponent  $n$ . It is interesting to note that in crushing problems with axisymmetric deformation modes, the circumferential extension and bending are present in equal proportions, leading to the term  $h^{1.5}$  in the expression for the crushing force, [4, 5, 7].

Using a semiempirical approach coupled with the modified "effective width" theory, Aya and Takahashi, [15] obtained the same exponent as in the formula (7.4). A larger value  $n = 1.86$  was suggested in [16] on purely empirical grounds while Magee and Thornton's fit of test result gave a smaller exponent  $n = 1.60$ , [17].

Introducing structural effectiveness  $\eta = P_m / A \sigma_0$  (non-dimensional crushing stress) and relative density  $\phi = A / A_1$  (solidity ratio) the formula (7.4) can be rewritten as

$$\eta = 0.948 \phi^{2/3} \quad (7.5)$$

where  $A_1 = C^2$  and  $A = 4hC$ .

The prediction of the preceding formula is shown in Fig. 8 by a dotted line. The present solution correlates well with experimental points, reported in [17] and follows rather closely the Magee and Thornton's empirical fit of the test results. Note, that in converting the experimental points to the dimensionless coordinate  $\eta - \phi$ , the ultimate stress was used in reference [17].

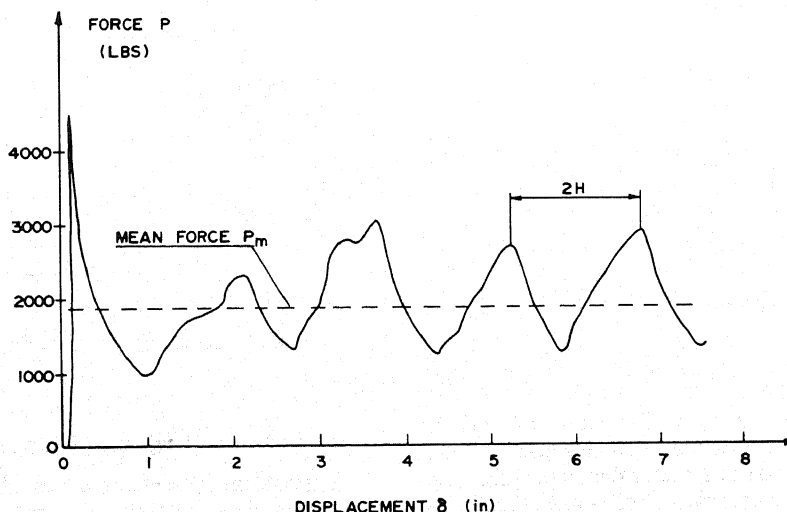


Fig. 7 Force-shortening characteristics of an axially compressed thin-walled column (courtesy of Ford Motor Co. Research Lab.)

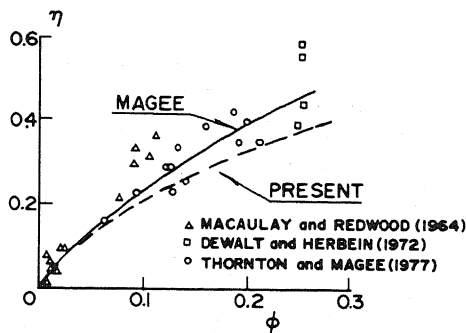


Fig. 8 Correlation between predicted and measured dimensionless crushing stress and relative thickness  $h/c$

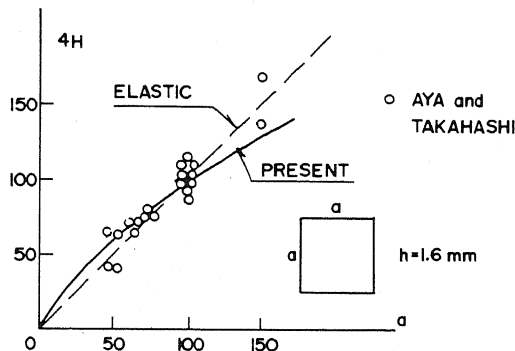


Fig. 9 Theoretical and experimental wavelength as a function of the column width

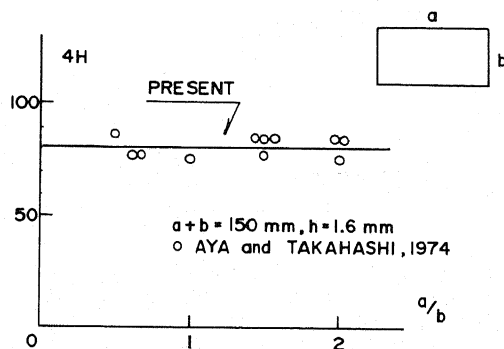


Fig. 10 Length of the folding mode versus the aspect ratio of rectangular cross section

Actually, for a work-hardening material, the plastic work should be related to an average flow stress  $\sigma_0$ . This average stress is much higher than the initial yield stress  $\sigma_y$  but is always below the ultimate stress  $\sigma_u$ . Taking in (7.5) as a reference stress a value that is smaller than  $\sigma_u$  would automatically raise all the experimental points.

At the same time the resulting discrepancies will be, to a large extent, offset by the fact that the actual distance over, while the force  $P_m$  exerts work, is  $2H-a$  rather than  $2H$ . Also, inclusion of a variable (increasing) thickness in extensional zones and retension of a small but finite parameter  $b/a$  would bring the  $\eta-\phi$  curve closer to experiments. As pointed out earlier, these effects were deliberately disregarded in the present analysis to offer a more clear interpretation of the crushing process and to derive a simple closed-form solution.

Perhaps an even more critical test for the validation of the present theory is to see how well it correlates with experimentally measured wavelength. This is shown in Fig. 9 and 10. The formula (7.2), which is now independent of  $\sigma_0$ , predicts correctly the height of the subsequent plastic folds in the entire range of  $h/C$  for which the folding process is progressive. The observation that for fixed  $(c+d)$ , both  $H$

and  $P_m$  do not depend on the aspect ratio  $c/d$  of the rectangular cross section is also featured by the present solution, Fig. 10.

## 8 Conclusions

The present analysis explains some important qualitative features of the crushing process of thin shells. It shows that plastic deformations of the magnitude exceeding by far those corresponding to the buckling or ultimate loads, are indeed confined to relatively small areas. The local curvature in these areas is relatively large, i.e., the radius of curvature  $b$  is small compared to a linear dimension  $C$ . The zones of extensional deformations are restricted to even smaller fraction of the total area of the shell but they always contribute to as much as one-third of the total energy dissipated in the structure. The remaining two-thirds of the energy results in equal proportions from inextensional deformations at stationary and moving hinge lines.

Calculations have shown that in all types of shells the mean crushing force depends markedly on the thickness of the shell ( $h^{5/3}$ ). At the same time the dependence on the linear dimension  $C$  is much weaker ( $C^{1/3}$ ). The present theory has also led to a good quantitative prediction of the mean crushing force and the associated collapse mechanism for axially compressed rectangular box columns.

The folding mode, developed in the paper has a potential of being used as a "special finite element" in numerical simulation of crash phenomena. This element could be used in the areas where sharp folds and wrinkles are formed to replace a necessarily dense and thus expensive finite element mesh.

The present methodology has been used in the calculation of the crushing strength of compressed and bent box columns with other cross-sectional shapes, for example closed hat-sections or channel sections. Some new results in this area can be found in reference [18]. Equally simple and accurate results were obtained for hexagonal cell structures and a relevant report will be released shortly, reference [19].

## 9 Acknowledgment

The work reported herein is a part of a research task No. J-F7F062P on "Structural Aspects of Vehicle Crash-worthiness" jointly undertaken by the Department of Ocean Engineering of the Massachusetts Institute of Technology and the Institute of Fundamental Technological Research in Warsaw. The financial support of the Polish Academy of Sciences and National Science Foundation through the Maria Curie-Skłodowska fund and the Massachusetts Institute of Technology is gratefully acknowledged. The authors are indebted to Dr. Henryk Stolarski for his interesting discussions on the subject and to Mrs. Ellen Ray for typing this manuscript.

## References

- 1 Johnson, W., Soden, P. D., and Al-Hassani, S. T. S., "Inextensional Collapse of Thin-Walled Tubes Under Axial Compression," *J. Strain Analysis*, Vol. 12, 1977, pp. 317-330.
- 2 Ohokubo, Y., Akamatsu, T., and Shirasawa, K., "Mean Crushing Strength of Closed-Hat Section Members," SAE Paper No. 740040.
- 3 Wierzbicki, T., and Akerstrom, T., "Dynamic Crushing of Strain Rate Sensitive Box Columns," SAE Paper No. 770592, *Proc. 2nd Int. Conf. Vehicle Struct. Mech.*, Southfield, Mich., Apr. 18-20, 1977.
- 4 Al-Hassani, S. T. S., Johnson, W., and Lowe, W. T., "Characteristics of Inversion Tubes Under Axial Loading," *J. Mechanical Engineering Sciences*, Vol. 14, 1972, pp. 370-381.
- 5 Alexander, J. M., "An Approximate Analysis of the Collapse of Thin Cylindrical Shells Under Axial Load," *Quart. J. Mechanics Applied Mathematics*, Vol. 13, 1969, pp. 10-15.
- 6 Morris, A. J., and Calladine, C. R., "The Local Strength of a Thin



Spherical Shell Loaded Radially Through a Rigid Boss," *Proc. 1st Int. Conf. on Pressure Vessel Technology*, ASEM, 1969.

7 de Oliveira, J. G., and Wierzbicki, T., "Crushing Characteristics of Rotationally Symmetric Plastic Shells," *J. Strain Analysis*, Vol. 17, 1982 (in print).

8 Kosinski, W., *Introduction to the Theory of Field Singularities and Wave Analysis*, (in Polish) Polish Scientific Publisher, Warsaw-Poznan, 1981.

9 Hopkins, H. G., "On the Plastic Theory of Plates," *Proceeding, Royal Society*, London, Series A, Vol. 241, 1957, pp. 153-179.

10 Hopkins, H. G., and Prager, W., "On the Dynamic of Plastic Circular Plates," *ZAMP*, Vol. 4, 1954, pp. 317-330.

11 Wierzbicki, T., "Crushing Analysis of Thin-Walled Structures," *Structural Mechanics Series*, Report No. 23, School of Engineering, Duke University, Feb. 1982.

12 Stolarski, H., "Dynamics of Strongly Deforming Rigid-Plastic Structures," Lecture notes prepared for the CISM Course on "Dynamics of Plastic Structures," Udine, Italy, Oct. 1979.

13 Abramowicz, W., and Sawczuk, A., "On Plastic Inversion of Cylinders," *Res. Mecanica Letters*, Nov. 1981.

14 Wierzbicki, T., "On the Formation and Growth of Folding Modes in Compressed Thin-Walled Structures," Paper offered for the IUTAM Symposium on Collapse: "The Buckling of Structures in Theory and Practice," University College London, Aug. 31-Sept. 3, 1982.

15 Aya, N., and Takahashi, K., "Energy Absorption Characteristics of Vehicle Body Structure," *Transactions of the Society of Automotive Engineers of Japan*, No. 7, May 1974.

16 Mahmood, H. F., and Paluszny, A., "Design of Thin Walled Columns for Crash Energy Management—Their Strength and Mode of Collapse," *Proc. 4th Instructional Conference on Vehicle Structural Mechanics*, Nov. 18-20, 1981, Detroit, pp. 7-18.

17 Magee, C. L., and Thornton, P. H., "Design Consideration in Energy Absorption by Structural Collapse," SAE Paper No. 780434, *Proc. Congress and Exposition*, Cobo Hall, Detroit, Mich., Feb. 27-Mar. 3, 1978.

18 Abramowicz, W., "Mechanics of the Crushing Process of Plastic Shells" (in Polish) Ph.D. Thesis, Institute of Fundamental Technological Research, Warsaw, Feb. 1981.

19 Wierzbicki, T., "Crushing Analysis of Metal Honeycombs," MIT Report #83-1, to appear in *Int. J. of Impact Engineering*, Vol. 1, No. 2, 1983.

## Readers Of The Journal Of Applied Mechanics Will Be Interested In:

### AMD-Vol. 55

#### Rotor Dynamical Instability

Ed. M. L. Adams, Jr.

Investigated is the current research that is being directed at obtaining a better interpretation of the interactive dynamical forces between rotor and stator other than the bearings. The Papers presented on this widely researched subject are: The Physical Nature of Rotor Instability Mechanisms; Labyrinth Seal Forces on a Whirling Rotor; Rotor Instability Cases in Large Steam Turbine Generators (Abstract); The Effects of Different Rub Models on Rotor Dynamics

(Abstract); Influence of Unbalance on the Stability Characteristics of Flexible Rotor Bearing Systems; Design Criteria for Improved Stability of Centrifugal Compressors; Measurement of Impeller Induced Rotor Forces (Abstract); Perturbation Tests of Bearing/Seal for Evaluation of Dynamic Coefficients; Case Studies of Rotor Instability in the Utility Industry.

1983 Bk. No. G00227/100 pages/\$24.00 list; \$12.00 members

Descriptions of other volumes of interest appear on pages 716, 739, 749, 776, 816, 862, 885, 890, and 911.

Address Orders To:

ASME Order Department • P.O. Box 3199, Grand Central Station • New York, N.Y. 10163

AM 109